J Mol Model (2009) 15:935–943
DOI 10.1007/s00894-008-0450-5

ORIGINAL PAPER

Theoretical study of 1-(4-hexylcyclohexyl)-4-isothiocyanatobenzene: molecular properties and spectral characteristics

Maciej Szaleniec · Renata Tokarz-Sobieraj · Wacław Witko

Received: 12 November 2008 / Accepted: 11 December 2008 / Published online: 27 January 2009

Abstract The mesogenic species 4-(4-hexylcyclohexyl) isothiocyanatobenzene (6CHBT) was studied with density functional theory and molecular mechanics in order to investigate the molecular properties, interactions between dimers and to interpret the IR spectrum. Two types of calculations were performed for model systems containing single and double molecules of 6CHBT. Calculations (involving conformation analysis) for isolated species indicated that the trans isomer, in the equatorial–equatorial conformation, is the most energetically stable. The 6CHBT molecule is polar, with a rather high (4.43 D) dipole moment with negatively charged isothiocyanato (NCS) ligand. The dimer–dimer interaction energies show that the head-to-head configuration (where van der Waals attraction forces play the major role) is the most energetically stable. Vibrational analysis provided detailed assignment of the experimental infra-red (IR) spectrum.

Keywords 4-(Trans-4-hexylcyclohexyl) isothiocyanatobenzene · Density functional theory · Infra-red · Van der Waals · Molecular mechanics

Dedication This paper is dedicated to the memory of Dr. Wacław Witko, who introduced us to research on mesogenic systems.

M. Szaleniec (✉) · R. Tokarz-Sobieraj
Institute of Catalysis and Surface Chemistry,
Polish Academy of Sciences,
ul. Niezapominajek 8,
30-329 Kraków, Poland
e-mail: ncszalen@cyf-kr.edu.pl

W. Witko
Henryk Niewodniczański Institute of Nuclear Physics,
Polish Academy of Sciences,
ul. Radzikowskiego 152,
31-342 Kraków, Poland

Introduction

The study of liquid crystals (LC) began in 1888 when F. Reinitzer observed two distinct melting points for cholesteryl benzoate. Due to their interesting properties [1–3], LC materials have found wide applications in technology, such as liquid crystal displays (LCDs) and LC thermometers, not to mention applications still under development such as LC optical imaging and recording devices [4, 5].

The present paper focusses on the 4-(4-hexylcyclohexyl) isothiocyanatobenzene (6CHBT) system, which belongs to the homologous series of 4-(4-alkylcyclohexyl) isothiocyanatobenzenes (nCHBT). 6CHBT, similar to other nCHBT molecules, forms a nematic LC. The sample of 6CHBT used here was synthesised by R. Dąbrowski at the Military University of Technology, Warsaw, Poland [6, 7]. In general, nCHBTs are characterised by low viscosity and high chemical stability, and appear to be an interesting component for display applications [8, 9]. Therefore, the physicochemical properties of 6CHBT have been studied experimentally by several groups [10–13]. Moreover, its application as a component of LC-doped magnetic materials has also been investigated [14–17]. Recently, its physicochemical properties were characterised using differential scanning calorimetry (DSC) and thermal polarising microscopy [18]. These experiments revealed the very interesting and complicated nature of the 6CHBT system. The heating history (i.e. the starting temperature) of the sample, and the heating rate in DSC experiments seems to influence the values of the double melting point of 6CHBT. The characteristic double melting peaks observed for samples precooled to 262–268 K join to form a single melting peak for samples precooled to temperatures above 269 K. Moreover, polarising microscopy suggested that the melting process is rather complex.

The main motivation for our research on 6CHBT was the expectation by the authors of the above-mentioned work that vibrational spectroscopy, supported by theoretical studies, will be helpful in solving the nature of the phenomena observed in DSC. It was suggested that structural interactions between 6CHBT molecules should exhibit two distinct and energetically separated modes that would explain the bimodal melting behaviour with its peculiar temperature dependency. Therefore, comparison of the IR spectra of isolated 6CHBT and its dimers with the experimental spectrum of the nematic phase should reveal some molecular interaction modes that could elucidate bimodal melting behaviour. To the best of our knowledge, our work is the first to provide density functional theory (DFT) level details on the molecular properties of this mesogenic system.

Methods

The studied model comprised the monomer and dimer assemblies of 1-(4-hexylcyclohexyl)-4-isothiocyanatobenzene. The 6CHBT molecule (see Fig. 1) is built of cyclohexane 1,4-disubstituted with an *n*-C_6H_{13} hydrocarbon chain and a 4-isothiocyanatobenzene moiety. We investigated both cis and trans isomers as well as all possible cyclohexane conformers (axial–equatorial, equatorial–axial and equatorial–equatorial, and axial–axial). Additionally, for the most stable geometry of the 6CHBT molecule, additional conformational studies were performed, i.e. the orientation of *then*-hexane, isothiocyanatobenzene and thiocyanate groups with respect to cyclohexane was varied. Moreover, contour plots of HOMO (Highest Occupied Molecular Orbital) and LUMO (Lowest Unoccupied Molecular Orbital) orbitals and electrostatic potential maps were obtained in GaussView 4.0.

Furthermore, the interaction of two 6CHBT molecules was investigated based on the structural data obtained for the analogous compound 11CHBT (Cambridge Crystallographic Data Centre CCDC 637960) [19]. Six different molecular contacts found in the 11CHBT crystal were used for simulation of possible 6CHBT interactions, namely: (1) two types of dimers in the head-to-head configuration, where the phenyl rings are in perpendicular assembly, with different extent of the overlap; (2) two types of tail-to-tail dimers with different extents of hydrocarbon chain overlap; (3) the head-to-tail dimer; and (4) two parallel 6CHBT molecules (for more details of geometric structures, see Results).

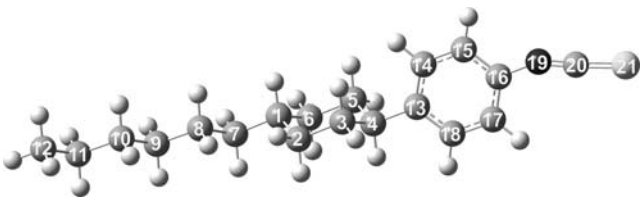

Fig. 1 The geometric structure of the trans isomer of 1-(4-hexylcyclohexyl)-4-isothiocyanatobenzene (6CHBT). Atoms are numbered *1–21*

All quantum chemical calculations were conduced in the Gaussian 03 suite of programs [20] with the B3LYP exchange-correlation functional [21]. Kohn-Sham orbitals were represented by linear combinations of atomic orbitals within the 6–31g(d) basis sets. A vibrational analysis was performed after each geometry optimisation in order to ensure that the minimum structural energy was reached, and also to simulate the IR spectrum, where frequencies were scaled by a factor of 0.9613 and zero point energy (ZPE) by a factor of 0.9804 [22]. The energies of the investigated dimers were corrected for base superposition errors (BSSE).

The van der Waals interactions (vdW) between dimers were evaluated with molecular mechanics (MM) calculations, which were performed with the augmented MM3 force field [23, 24] in the Cache Pro 7.5 package. In order to calculate the value of vdW attraction, the energy of the dimers was scanned in the range of 10 Å to 2.5 Å in steps of 0.3 Å, taking the long distance energy as a reference. For each scan point, the geometries of the models were optimised (up to 1,000 iterations), updating vdW forces every tenth iteration. Finally, the MM energy for distance found in the DFT calculation was used in further analysis.

Results

Isomer configurations

The substitution of cyclohexane in the 1,4 positions leads to formation of two isomers: cis and trans. Each isomer can adopt two conformations, namely axial–equatorial (ae) and equatorial–axial (ea) for the cis isomer, and equatorial–equatorial (ee) and axial–axial (aa) for the trans isomer. In all cases, the second letter describes the position of the *n*-hexane substituent whereas the first letter indicates the location of isothiocyanatobenzene.

The results of calculations (Fig. 2) are in agreement with experimental data indicating the ee conformer as the most stable, followed by ae, ea, and finally aa. The energy difference between trans conformers (ee and aa, 24.35 kJ mol^{-1}; ZPE 26.99 kJ mol^{-1}) is larger than for cis conformers (ae and ea, 6.37 kJ mol^{-1}; ZPE 6.75 kJ mol^{-1}). These results show that, for a pure trans isomer (ee and aa) at 298 K, more than 99.9% of 6CHBT molecules would be in the ee conformation. In the case of a pure cis isomer (ae and ea) the Boltzman distribution indicates domination of the ae conformer (91.8 %).

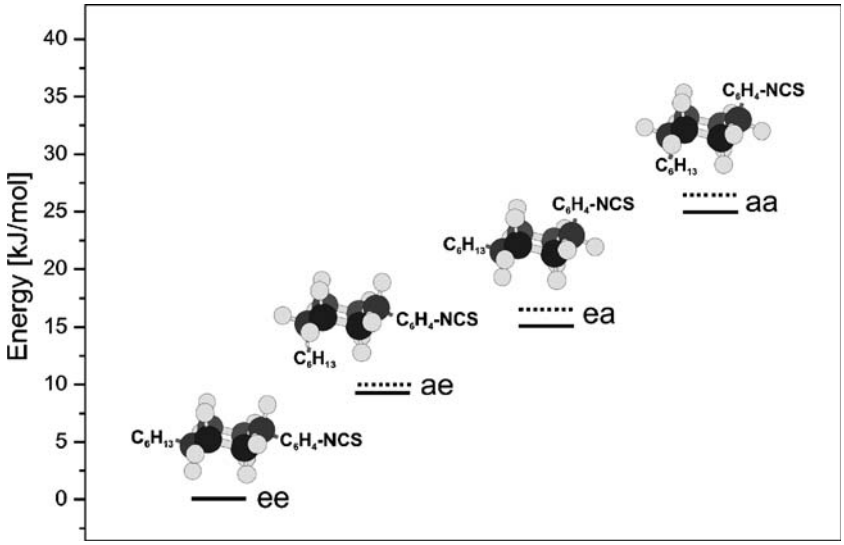

Fig. 2 The relative energy of different 6CHBT conformers. *Solid lines* Energy differences, *dotted lines* zero point energy (ZPE) corrected energy differences. *ae* Axial–equatorial, *ea* equatorial–axial, *ee* equatorial–equatorial, *aa* axial–axial

This result is in perfect agreement with structural studies on the condensed mesogenic phase [19], where the trans ee conformer is the main component. Furthermore, if one assumes that these energy differences influence the synthesis of 6CHBT, and that all conformers are available in the Boltzmann distribution, the ee conformer would form 97.201% of the total number of molecules (2.564% ae, 0.230% ea, 0.005% aa). Indeed, this is again in accordance with experiment results, as mainly the trans isomer is produced during synthesis and naturally attains the low energy ee conformation (R. Dabrowski, personal communication).

Additional conformational studies were performed for the most stable ee geometry of the 6CHBT molecule. The dihedral angles between the *n*-hexane carbon backbone and the cyclohexane ring (8–7–1–2), as well as the dihedral angle between the isothiocyanatobenzenene plane and cyclohexane (3–4–13–14), were scanned (in 15° steps).

The scan of the (8–7–1–2) dihedral angle between *n*-hexane and cyclohexane reveals three minima (see Fig. 3) for each position in staggered conformation of 1, 8 atoms. The two deepest, symmetrically equivalent minima are found at −171.0° and −61.0°, where the *n*-hexane chain is oriented sideways to the cyclohexane ring. These minima are separated by a rotation barrier equal to 9.2 kJ mol^{-1}. The third minimum is found at 64°, where the *n*-hexane chain is pointing upwards. The rotational barrier between the deepest and the 64° minimum is 20.5 kJ mol^{-1} (Fig. 3).

The scan of the (3–4–13–14) dihedral angle reveals two isoenergetic minima (see Fig. 4) at 116.6° and −63.4°, where isothiocyanatobenzene is perpendicular to the plane of cyclohexane, with the value of the rotation barrier equal to 11.7 kJ mol^{-1}. Rotation of the non-crystallographic-similarity (NCS) ligand along the C15–C16–N19–C20 dihedral angle leads to two energetic and geometric minima equivalent to those mentioned above with just a slightly smaller rotation barrier of 5.44 kJ mol^{-1}.

The obtained conformation for 6CHBT is very similar to the experimental conformation of the hydrocarbon chain found in the 11CHBT crystal structure. The experimental (8–7–1–2) dihedral angle for 11CHBT is −58°, while calculated value for 6CHBT is −61.0°. However, for the (3–4–13–14) dihedral angle a higher value of −93° is observed experimentally for 11CHBT, compared to that found in ab initio calculations (−63.4°). This seems to be due to intermolecular

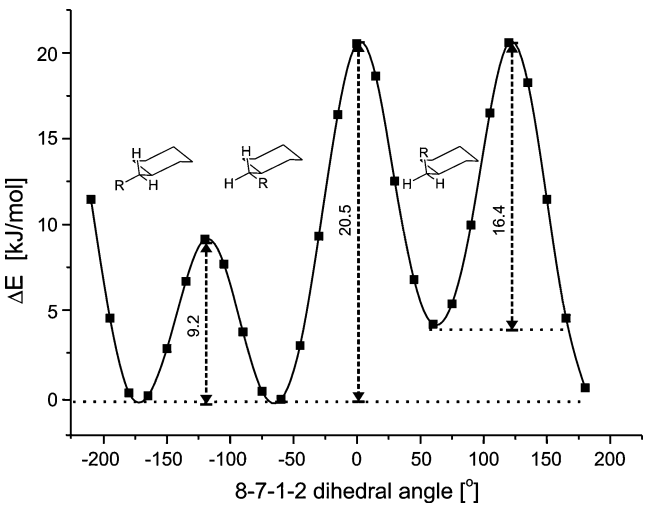

Fig. 3 Energy scan along the 8–7–1–2 dihedral angle revealing three minima. The schemes depict the type of conformer; *R* hydrocarbon chain

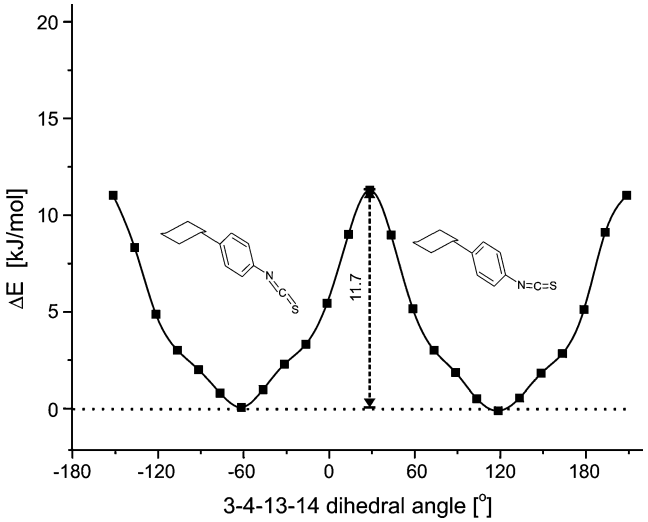

Fig. 4 Energy scan along the 3–4–13–14 dihedral angle revealing two equivalent minima

interactions in the condensed phase, as the phenyl rings tend to adopt a mutually perpendicular arrangement. This was additionally confirmed by intermolecular contact studies (see dimer 2 in the section on Intermolecular contacts below). When molecules in the head-to-head configuration are pulled closer together, the isothiocyanatobenzene ring starts to rotate along the 3–4–13–14 dihedral angle (starting from −60° at a distance of 10 Å) resulting in a tilted conformation with a dihedral angle equal to −92.7° at 2.8 Å.

As in 11CHBT, the 6CHBT thiocyanato group is almost linear (the N=C=S angle is 176° in both structures) , and always in-plane with the aromatic ring. Also similar are the C (from benzene ring)–N, N=C and C=S bond lengths , which are equal to 1.38 Å, 1.20 Å and 1.59 Å in 6CHBT and 1.40 Å, 1.14 Å and 1.54 Å in 11CHBT, respectively. However, in contrast to experimental crystallographic data for 11CHBT [where the C(16)-N=C equals 168°], the calculated C(16)-N=C angle in 6CHBT structure is 154°.

Searching the Cambridge Crystallographic Database for structures containing an isothiocyanatobenzene fragment revealed 14 compounds with a non-coordinating NCS group. Analysis of the geometry showed that the C (benzene)-N=C angle spans from 139.4° up to 172.5°, with an average value of 158.3°, while the N=C=S angle is equal to 173.7° on average. The average lengths of the C–N, N=C and C=S bonds are 1.40 Å, 1.19 Å and 1.56 Å, respectively, which is in very good agreement with bond lengths calculated for 6CHBT. The closest structural analogue of 11CHBT and 6CHBT found was 1-hexyl-4-(4-isothiocyanatophenyl)bicyclo(2.2.2)octane (CCDC: OGIBIP) [25], where the C(benzene)-N=C angle equals 152.2°, which is very close to that calculated for 6CHBT. It can be concluded that the NCS ligand is usually more bent than in 11CHBT, but such straight configurations are not exceptional. One cannot exclude that, as suggested by Mandal et al. [19], in the condensed phase of nCHBT LCs, the N–C atomic bond attains a partially triple character resulting in a straight isothiocyanate configuration.

Electronic properties of the isolated molecule

Analysis of the frontier orbital distribution shows that both HOMO and LUMO are localised mainly at phenyl ring and thiocyanato groups, with small a contribution from cyclohexane atoms (Fig. 5). The energy difference between both frontier orbitals (LUMO−HOMO) is 480.7 kJ mol^{-1}. The approximate electron affinity (εLUMO) and the ionisation potential (εHOMO) are 107.5 kJ mol^{-1} and

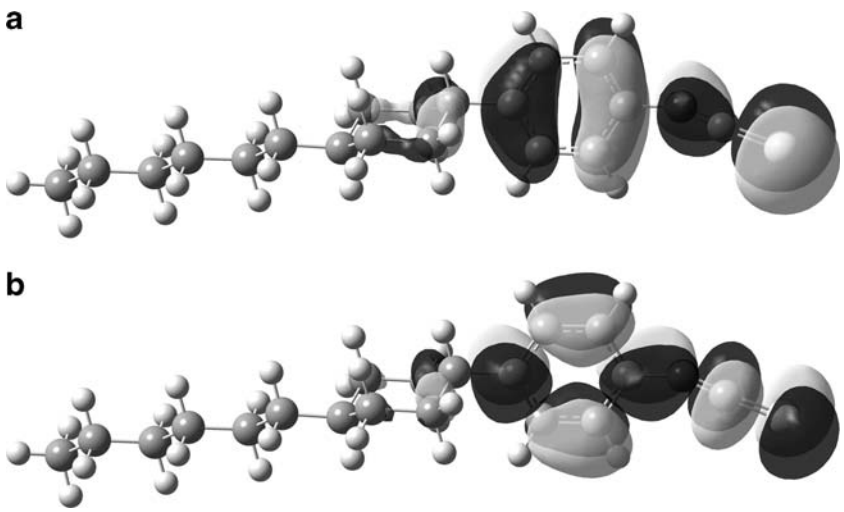

Fig. 5a,b The shape of 6CHBT frontier orbitals. **a** HOMO (highest occupied molecular orbital), **b** LUMO (lowest unoccupied molecular orbital)

588.2 kJ mol^{-1}, respectively. These results show that it is very hard to ionise the 6CHBT molecule, explaining its high chemical stability.

6CHBT exhibits a strong dipole moment (4.43 D) that is parallel to the ring plane and points in the direction of the hydrocarbon chain. This strong polarity of the molecule can be depicted with the electrostatic potential mapped on the electron density isosurface (Fig. 6). Analysis of electrostatic potential (ESP) distribution shows that the head of the molecule exhibits strong negative potential (indicating the accumulation of negative charge on the electrophylic heteroatoms), and mildly negative potential above and below the aromatic ring plane (due to the accumulation of π electrons). However, the edges of the aromatic ring have a positive potential. As can be expected, the potential of the rest of the hydrocarbon chain is roughly neutral. Such a distribution of ESP suggests that 6CHBT molecules will be involved in face-to-edge electrostatic interactions with their aromatic rings as well as edge-to-NCS interactions (see below).

Intermolecular contacts

Next, the interactions of two isolated molecules were studied. Taking the 11CHBT crystallographic structure [19] as a model, six different types of molecular associations were constructed and their geometries were optimised on a DFT level (Fig. 7).

Dimer 1 Molecules 1 and 2—head-to-head configuration where the phenyl rings are almost in perpendicular position and the isothiocyanatobenzene groups overlap;

Dimer 2 Molecules 1 and 4—head-to-head configuration where the phenyl rings are in perpendicular position and the thiocyanatho (NCS) groups overlap with cyclohexane rings;

Dimer 3 Molecules 1 and 3—head-to-tail configuration where both molecules lie almost along the long axis and the thiocyanato group faces the end of the hydrocarbon chain of the other molecule;

Dimer 4 Molecules 2 and 3—tail-to-tail configuration where the end of hydrocarbon chain of one molecule overlaps the cyclohexane ring of another molecule;

Dimer 5 Molecules 3 and 4—tail-to-tail configuration with overlapping hydrocarbon chains;

Dimer 6 Molecules 2 and 4—two parallel molecules, located exactly one above the other.

Table 1 lists the contact interaction energies ΔE, corrected for BSSE (E+BSSE). ΔE is defined as the difference between the energy of two interacting molecules (BSSE-corrected) and sum of the energies of two isolated molecules. Interaction energies were negative only for head-to-head configurations. Larger interaction energy (−2.51 kJ mol^{-1}) is observed for dimer 1, which involves interactions of two isothiocyanatobenzene groups, than for dimer 2 (−0.79 kJ mol^{-1}), where the two thiocyanato groups interact with cyclohexane rings. For other dimers, a small repulsion is observed (ranging from 0.67 to 3.72 kJ mol^{-1}). The largest repulsive effect was found for the two 6CHBT molecules located exactly one above the other.

It is known that DFT approximation does not describe correctly long-range intermolecular interactions such as vdW forces [26]. In order to estimate this part of the intermolecular energy, molecular mechanics calculations with the MM3 force field were conducted. Table 1 summarises all intermolecular contributions to energy obtained from MM3, namely vdW interactions (ΔvdW), hydrogen bond interactions (ΔH bond) and electrostatic interactions (Δelect). For each DFT-level optimal geometry, MM3 optimisation was performed with frozen selected distance coordinates (distance r for each dimer is given in Table 1 and Fig. 7). The reference energies (where no interactions take place) were obtained for two 6CHBT molecules separated by 10 Å (along the selected r coordinate). This ensures that the energies obtained from MM correspond to the dimer geometries from DFT, even if the structures of individual 6CHBT molecules are optimised within each theory. As a result, the MM energies provide additional information to that obtained from DFT.

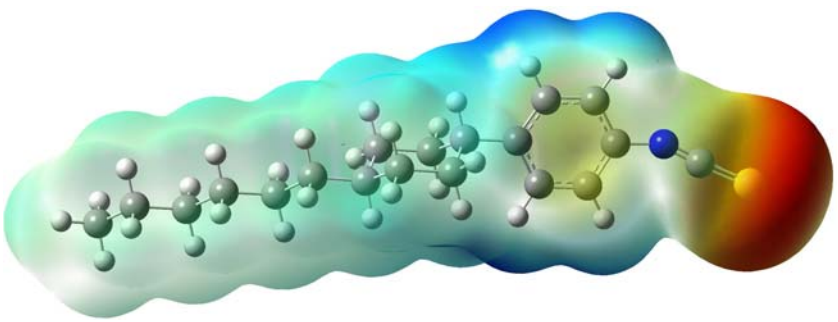

Fig. 6 Electrostatic potential (ESP) mapped onto electron density map. *Red* Negative potential, *blue* positive potential

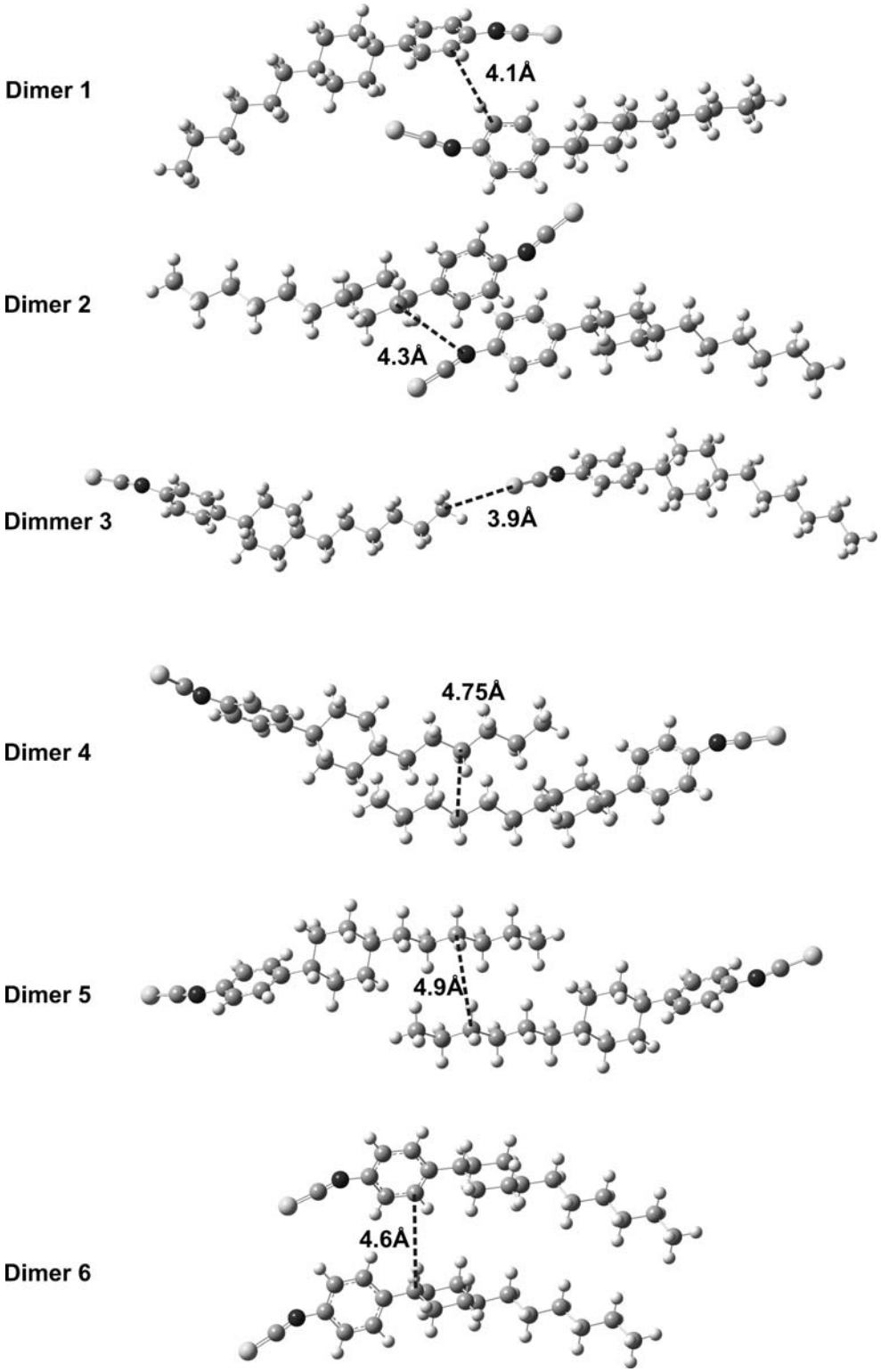

Fig. 7 The density functional theory (DFT) optimised geometry of all studied dimmers. *Dashed lines* Selected distance coordinate that was frozen for molecular mechanics (MM3) optimisation

As expected, the results of the calculations show that there are no hydrogen bonds between 6CHBT molecules. The small values (from −1.21 to −2.18 kJ mol^{-1}) observed for dimers 4, 5 and 6, are connected to the overlapping of hydrocarbon chains of both molecules and interactions of a large number of hydrogen atoms from the C_6H_{13} parts. Therefore, as such, these cannot be treated as hydrogen bond interactions.

For most 6CHBT molecules the electrostatic energies are negligible. However, for dimers 1 and 2, small attractive interactions (−0.96 and−1.76 kJ mol^{-1}, respectively) are found. It seems that this attractive interaction is due to the

Table 1 Summary of interaction energies for dimer interaction between 4-(4-hexylcyclohexyl) isothiocyanatobenzene (6CHBT) molecules calculated with the B3LYP density functional theory (DFT) and molecular mechanics (MM3) methods. *ΔE B3LYP* Energy difference between dimer and two isolated 6CHBT molecules, *ΔvdW* van der Waals interactions, *Δ(H bond)* hydrogen bonds interactions, *Δ(elect)* electrostatic interaction, *Δ(intra)* intermolecular interactions (vdW+H-bonding+electrostatic), *Total* sum of ΔE B3LYP and Δ(intra)

Type of contact	DFT		MM3				Total
	r [Å]	ΔE B3LYP[kJ mol^{-1}]	Δ(vdW)	Δ(H bond)	Δ(elect)	Δ(intra)	
Dimer 1 (molecules 1,2)	4.1	−2.51	−14.48	0.67	−0.96	−14.77	−17.28
Dimer 2 (molecules 1,4)	4.3	−0.79	−13.05	0.33	−1.76	−14.43	−15.23
Dimer 3 (molecules 1,3)	3.9	0.67	−0.92	0.04	0.00	−0.88	−0.21
Dimer 4 (molecules 2,3)	4.75	2.51	−8.54	−2.18	0.04	−10.71	−8.20
Dimer 5 (molecules 3,4)	4.9	1.97	−5.82	−1.21	0.00	−7.03	−5.06
Dimer 6 (molecules 2,4)	4.6	3.72	−14.98	−1.51	−0.25	−16.74	−13.01

overlap of the highly polar thiocyanato group with the phenyl ring.

The intermolecular interactions between two 6CHBT molecules come mainly from vdW interactions. As expected, the largest vdW energy is observed for dimers with the largest molecular overlap. The biggest effect (−14.98 kJ mol^{-1}) is observed for dimer 6 (two parallel 6CHBTs), where the length of the molecular overlap is ca. 15 Å. The head-to-head configurations exhibit only slightly smaller vdW attraction (−14.48 for dimer 1 and −13.05 for dimer 2) even though the extent of the molecular overlap is in the range of 8–9 Å. For dimers 4 and 5, where the molecular overlaps were ca. 8 Å and 6.5 Å, respectively, the vdW interaction energies are equal to −8.54 and −5.82 kJ mol^{-1}. Finally, for dimer 3, where no molecular overlap takes place, the smallest vdW attraction is found, namely−0.92 kJ mol^{-1}. These results show that: (1) vdW interaction of the dipolar isothiocyanatobenzene group is stronger than the interaction of apolar hydrocarbon chains, and (2) the magnitude of vdW attraction is proportional to the extent of the molecular overlap (due to the additive character of the vdW interaction).

One can roughly estimate the overall interaction energy by summing ΔE B3LYP and MM intermolecular energy Δ(intra). Of course, such an approach is an approximation as both methods correctly address the electrostatic interaction, which results in double counting of the electrostatic effects in case of dimers 1 and 2. Nevertheless, it shows which contacts may be the most favourable and, as a result, most likely to exist in the nematic phase. As can be seen from Table 1, the most favorable interaction energies (−17.28 and −15.23 kJ mol^{-1}) are found for both head-to-head configurations (dimers 1 and 2). The parallel configuration (dimer 6) exhibits a total interaction energy of −13.01 kJ mol^{-1} followed by dimers 4 and 5 (−8.20 and −5.06 kJ mol^{-1}). The head-to-tail interaction energy turns out to be close to zero. These results point to the head-to-head configuration being the most likely to exist in the nematic phase, which is in agreement with conclusions drawn for 11CHBT by Mandal et al. [19].

IR spectrum

In order to cross-validate the results of ab initio modelling, the IR spectrum for the geometry of the most stable 6CHBT conformer was calculated. As any significant difference in the single molecule spectrum between experimental and calculated results might indicate important intermolecular interactions, the same analysis was performed for all studied contacts.

The resulting spectrum matched very nicely the experimental one, and allowed assignment of the main bands (see Fig. 8). The strongest bands, in the range of 2,900–3,000 cm^{-1}, come from the symmetric and asymmetric stretching modes of sp^3 hydrocarbon, with the highest band at 2,922 cm^{-1} coming from asymmetric C–H bond stretching in both cyclohexane and CH_2 groups of *n*-hexane. The highest band in the spectrum is observed at 2,075 cm^{-1} and was identified as a stretching of the C=N bond in the NCS group. In the theoretical single molecule spectrum, this band is very high and narrow, while in the experimental one it is very wide, suggesting various interactions involving the NCS group that broadens the peak (Fig. 8a).

Another strong peak at 1,505 cm^{-1} is associated with deformations of the aromatic ring that alternately contracts pairs of C13–C14, C13–C18 and C16–C15 and C16–C17 bonds, rocking the aromatic hydrogen atoms in the plane of the aromatic ring.

The accompanying bands around 1,450 cm^{-1} are associated with scissor deformations of C–H_3 and C–H_2 groups. The band at 934 cm^{-1} is associated with the characteristic 'ring breathing' C=C stretching mode, which also involves elongation of the C20=S21 bond. The peak at

828 cm^{-1} can be assigned to out-of-plane bending of the aromatic hydrogen atoms and, finally, the 536 cm^{-1} band can be associated with either in-plane bending of the NCS group or out-of-plane bending of the aromatic ring.

As mentioned before, the ν_s^{NCS} band in the experimental spectrum is very wide. In order to explain this, the IR spectra of possible contacts were obtained. The shifts in the ν_s^{NCS} band position are listed in Table 2 along with changes to the δ^{NCS} deformation band (which also depict changes in NCS electronic environment).

The observed shift in the ν_s^{NCS} of dimer 1 (energetically favorable) partially explains the width of the band in the experimental spectrum. Dimer 1 also has the strongest shift of δ^{NCS}. Interestingly, similar shifts are not observed for another head-to-head configuration (dimer 2). Apparently, this shift is associated with the mode of NCS interaction with the aromatic ring.

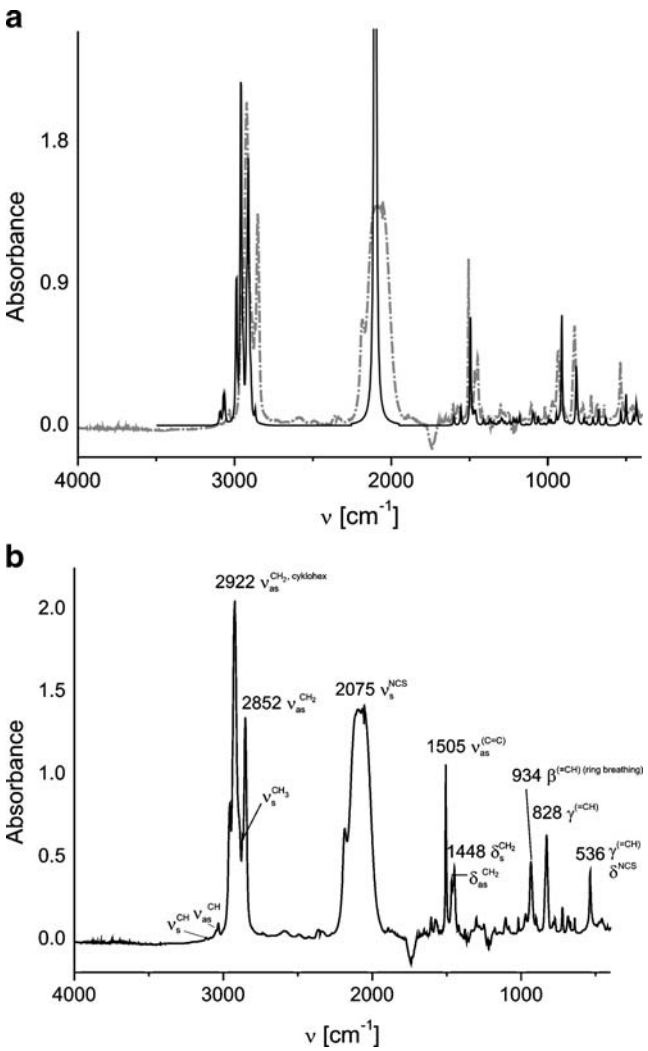

Fig. 8a,b Infra-red (IR) spectra of 6CHBT. **a** Overlay of experimental (*dotted grey line*) and calculated (*solid black line*) spectrum, **b** peak assignment of experimental spectrum based on theoretical calculations

Table 2 Frequencies of non-crystallographic-similarity (NCS) band deformation in isolated and dimer models

Type of contact	ν_s^{NCS}[cm^{-1}]	δ^{NCS} [cm^{-1}]
Isolated molecule	2,102	500
Dimer 1	2,127 and 2,119	476
Dimer 2	2,099 and 2,100	487
Dimer 3	2,109	480
Dimer 4	2,101	489 and 499
Dimer 5	2,100 and 2,002	489 and 500
Dimer 6	2,098 and 2,103	487 and 489

The results of our calculations show that no hydrogen bonds are created in the studied 6CHBT systems, as no batochromic shift was observed along with the increase in band intensity of the IR spectrum. This was to be expected, as the potential hydrogen bond donor–acceptor distances in the studied dimers are well above 3 Å, and no significant hydrogen bonding interaction was found by MM calculations.

Conclusions

The results of calculations show that 1-(trans-4-hexylcyclohexyl)-4-isothiocyanatobenzene in ee conformation is the most energetically stable of all possible isomers of 6CHBT. This explains the selectivity of 6CHBT synthesis towards the trans product.

Detailed conformational analysis proves that the most stable geometry of the 6CHBT molecule in the gas phase is the one with the isothiocyanatobenzene ring plane perpendicular to the cyclohexane ring plane, and with the *n*-hexane chain pointing sideways to the cyclohexane ring (in staggered alignment). Two possible rotamers for the NCS ligand are energetically equivalent to conformers involving rotation of the isothiocyanatobenzene ring, with the rotational barrier for the former process being smaller than the latter by 5.44 kJ mol^{-1}.

Analysis of frontier orbital electronic density distributions shows that both HOMO and LUMO orbitals are localised mainly at the phenyl ring and the thiocyanato group, with small contributions from atoms of cyclohexane. 6CHBT is a polar molecule with the head exhibiting negative electrostatic potential and an apolar hydrocarbon tail. As a result, it possesses a strong dipole moment (4.43 D) that is parallel to the ring plane and points in the direction of the hydrocarbon chain. Moreover, the high value of the ionisation potential (−ε HOMO) explains the high chemical stability of 1-(trans-4-hexylcyclohexyl)-4-isothiocyanatobenzene.

vdW interactions are the predominant attractive forces present in the condensed phase of the studied system.

Hydrogen bonds are not observed and the electrostatic interactions are relatively small. The head-to-head configuration is the most energetically favourable among the studied dimers.

The theoretical IR spectrum of the isolated 6CHBT molecule is in good agreement with the experimental spectrum and facilitates assignment of specific IR bands. The experimentally observed broadening of the ν_s^{NCS} band can be explained by the shift in the IR spectrum of the most energetically favourable head-to-head dimer (dimer 1).

Unexpectedly, our theoretical studies do not explain the intricate melting behaviour of 6CHBT observed by Witko et al. [18].

Acknowledgement The Ministry of Science and Higher Education supported this research under computational grants MNiSW/SGI3700/PAN/003/2007 and KBN/SGI2800/PAN/037/2003.

References

1. Chandrasekhar S, Madhusudana NV (1980) Annu Rev Mater Sci 10:133x
2. Meyer RB (1977) Mol Cryst Liq Cryst 40:33
3. de Gennes PG, Prost J (1995) The physics of liquid crystals. Oxford University Press, Oxford
4. Okabe M Polymer dispersion liquid crystal recording medium and method and apparatus for reproducing information. United States Patent 5933201
5. Hansen JR, Schneeberger RJ (1968) IEEE Trans Electron Devices 15:896
6. Dąbrowski R, Dziaduszek J, Szczuciński T (1984) Mol Cryst Liq Cryst Lett 102:155
7. Baran JW, Raszewski Z, Dąbrowski R, Kędzierski J, Rutkowska J (1985) Mol Cryst Liq Cryst 123:237
8. Dabrowski R, Dziaduszek J, Szczucinski T (1985) Mol Cryst Liq Cryst 124:241
9. Bauman D, Chrzumnicka E, Mykowska E, Szybowicz M, Grzelczak N (2005) J Mol Struct 744–747:307
10. Balcerzak A (2005) Mol Quan Acoust 26:7
11. Bogoslovov RB, Roland CM, Czub J, Urban S (2008) J Phys Chem B 112:16008
12. Raszewski Z, Kedzierski J, Rutkowska J, Zieliski J, Mija J, Dabrowski RD, Opara T (1993) Liq Cryst 14:1959
13. Jadzyn J, Hellemans L, Czechowski G, Legrand C, Douali R (2000) Liq Cryst 27:613
14. Kopčanský P, Potočová I, Koneracká M, Timko M, Jansen AGM, Jadzyn J, Czechowski G (2005) J Magn Magn Mater 289:101
15. Tomašovičová N, Kopčanský P, Koneracká M, Tomčo L, Závišová V, Timko M, Éber N, Fodor-Csorba K, Tóth-Katona T, Vajda A, Jadzyn J (2008) J Phys: Condens Matter 20:204123
16. Kopanský P, Koneracká M, Timko M, Jadzyn J (2005) Phys Status Solidi (b) 243:317
17. Kopcanský P, Tomasovicová N, Koneracká M, Závisová V, Timko M, Dzarová A, Sprincová A, Eber N, Fodor-Csorba K, Tóth-Katona T, Vajda A, Jadzyn J (2008) Phys Rev E 78:011702
18. Witko W, Padoł AM, Zieliński PM (2007) Phase Trans 80:717
19. Biswas S, Haldar S, Mandal PK, Goubitz K, Schenk H, Dabrowski R (2007) Cryst Res Technol 42:1029
20. Frisch MJ, Trucks GW, Schlegel HB, Scuseria GE, Robb MA, Cheeseman JR, Montgomery JA Jr, Vreven T, Kudin KN, Burant JC, Millam JM, Iyengar SS, Tomasi J, Barone V, Mennucci B, Cossi M, Scalmani G, Rega N, Petersson GA, Nakatsuji H, Hada M, Ehara M, Toyota K, Fukuda R, Hasegawa J, Ishida M, Nakajima T, Honda Y, Kitao O, Nakai H, Klene M, Li X, Knox JE, Hratchian HP, Cross JB, Adamo C, Jaramillo J, Gomperts R, Stratmann RE, Yazyev O, Austin AJ, Cammi R, Pomelli C, Ochterski JW, Ayala PY, Morokuma K, Voth GA, Salvador P, Dannenberg JJ, Zakrzewski VG, Dapprich S, Daniels AD, Strain MC, Farkas O, Malick DK, Rabuck AD, Raghavachari K, Foresman JB, Ortiz JV, Cui Q, Baboul AG, Clifford S, Cioslowski J, Stefanov BB, Liu G, Liashenko A, Piskorz P, Komaromi I, Martin RL, Fox DJ, Keith T, Al-Laham MA, Peng CY, Nanayakkara A, Challacombe M, Gill PMW, Johnson B, Chen W, Wong MW, Gonzalez C, Pople JA (2004) Gaussian 03 revision D01. Gaussian Inc., Wallingford CT
21. Becke AD (1993) J Chem Phys 98:5648
22. Foresman JB, Frisch AE (1996) Exploring chemistry with electronic structure methods, 2nd edn. Gaussian Inc., Pittsburgh, PA
23. Allinger NL, Yuh YH, Lii J-H (1989) J Am Chem Soc 111:8551
24. Lii J-H, Allinger NL (1989) J Am Chem Soc 111:8576
25. Lokanath NK, Revannasiddaiah D, Sridhar MA, Prasad JS (2001) Mol Cryst Liq Cryst 364:703
26. Grimme S (2004) J Comput Chem 12:1463